TÜBİTAK

Turkish Journal of Physics

http://journals.tubitak.gov.tr/physics/

Research Article

Turk J Phys
(2018) 42: 146 – 156

doi:10.3906/fiz-1706-28

Control of laser-induced nonadiabatic molecular alignment in dissipative media

Gamze KAYA[1,2,*]

[1]Department of Physics, College of Science, Texas A&M University, College Station, TX, USA
[2]Department of Electric and Energy, Vocational School of Technical Sciences, Çanakkale Onsekiz Mart University, Çanakkale, Turkey

Received: 22.06.2017 • **Accepted/Published Online:** 22.11.2017 • **Final Version:** 26.04.2018

Abstract: Laser-induced nonadiabatic alignment in nitrogen and mixtures of nitrogen with Ar gas was investigated using the ultrafast optical Kerr effect in the collinear pump–probe setup. We find that dissipative media produce desired alignment characteristics in distinct manners to decoherence and to population relaxation. The results show that the intense laser alignment can be used as a control tool of molecular dynamics in dissipative environments.

Key words: Atomic and molecular physics, nonadiabatic molecular alignment, ultrafast nonlinear optics, femtosecond phenomena, ultrafast measurements

1. Introduction

In nonadiabatic alignment in which the laser pulse duration is less than the characteristic molecular rotational period, the short laser pulse creates a rotational wave packet, i.e. a coherent superposition of the rotational states in each molecule after the laser pulse has left [1]. Studies on nonadiabatic molecular alignment (see [2,3]) provide a variety of applications, such as chemical reaction control [4], selectively controlled alignment of isotopes [5], molecular structure imaging [6], pulse compression [7], and quantum information processing [8].

Femtosecond laser systems with advanced technology enable one to align molecules and observe the molecular dynamics by using a pump–probe technique [9]. Here an initial pump pulse induces the formation of a dynamically anisotropic medium that will dephase and rephase in time, and after that simultaneous variations in the interaction between such a medium and a probe pulse can be detected through different processes such as ionization [1,10–12], fragmentation [13,14], and high harmonic generation [6,15–18] or by spatial and spectral modulation of the probe pulse [19–23].

The pump–probe photoionization approach is one of the variety of detection methods for studying spectroscopy of the rotational states offered by rotational coherence spectroscopy [24], which is based on rotational quantum beats that result from the coherent excitation of rotational levels. Earlier transient birefringence caused by the time evolution of a coherent superposition of rotational states induced by a laser field was used for their observation [25]. Since the significant studies on the theory [26,27] and the first experimental results of nonadiabatic molecular alignment [28], this fascinating phenomenon continues attracting considerable interest from researchers. The degree of alignment was measured by a weak field polarization technique based on Raman scattering [29]. To monitor rotational dynamics, the depolarization of the probe pulse due to transient birefringence resulting from nonadiabatic alignment was also studied [30]. In another study, the coherences of

*Correspondence: gamzekaya@comu.edu.tr

the molecular rotational dynamics caused by the dynamic Stark effect and stimulated Raman scattering were examined in detail by refractive index modulation [31].

In the very high sensitivity of the collinear pump–probe setup, the collinearly propagating pump and probe beams provide much better sensitivity under our experimental conditions and so we investigate laser-induced nonadiabatic alignment in nitrogen and mixtures of nitrogen with Ar gas using ultrafast optical Kerr effects to control decays and decoherences of the alignment to some degree.

2. Experimental setup

The standard version of the setup in Refs. [22,32], in which the pump and probe beams propagate collinearly and are discriminated spectrally rather than spatially, was used successfully for measurements at room temperature. Aside from easier adjustment, the setup has the additional advantage of providing a large interaction volume even for lenses with relatively short focal length. It can thus combine high intensity with high sensitivity. As shown in Figure 1, our experiments were carried out with a Ti:sapphire amplified laser system (pulse duration of $\sim$50 fs, central wavelength of 800 nm, and an output energy of 1 mJ per pulse (split between pump and probe beams) at a 1 kHz repetition rate). The time delay between the linearly polarized pump and probe pulses was precisely adjusted (0.66 fs) using a translational stage controlled by a stepping motor (GTS150, ESP300, Newport). The recombined pump and probe beams were then focused into a gas cell of 85 cm that was filled with pure nitrogen gas with the pressure up to 4 bars by using a lens with a focal length of f = 60 cm. For the nitrogen–argon gas mixture where a constant partial pressure of nitrogen of 1 bar was diluted by a partial pressure of argon of 2 bars, we performed measurements of alignment decay at room temperature. Experimentally, the nature of the signal of aligned molecules depends on the time delay between the pump and probe laser pulses, and so at the exit of the gas cell the white-light signals were measured simultaneously after the cell as seen in Figure 1.

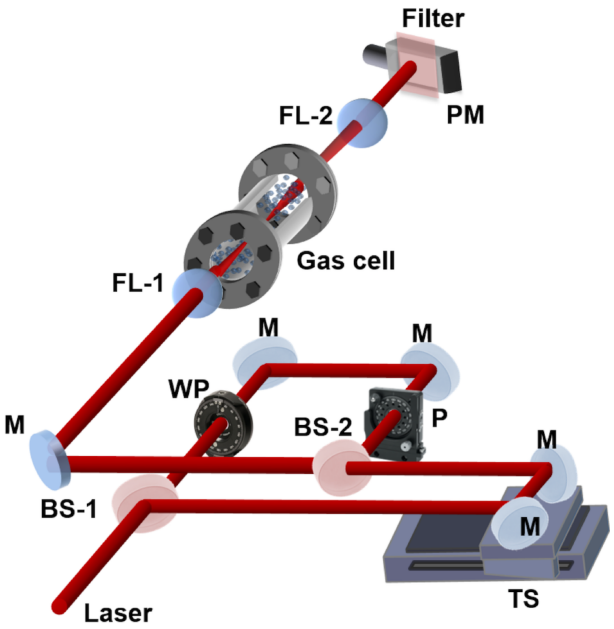

Figure 1. The schematic of the experimental setup. BS: beam-splitters, TS: translational stage, WP: wave plate, P: polarizer, M: flat mirrors, FL: focusing lens, and PM: power meter.

3. Theory

Far away from any resonance the potential that a linear molecule experiences in a rapidly alternating field is described as [3] $H_{int}(t) = -1/2(\Delta\alpha\cos^2\theta + \alpha_\perp)\langle E^2(t)\rangle$. Here $E(t)$ is the amplitude of the electric field, θ is the angle between the molecular axis and the polarization direction of the field; $\Delta\alpha$ and $\alpha_\perp$ are anisotropic polarizability of the molecule and polarizability perpendicular to the molecular axis, respectively. The rotational alignment of a linear diatomic molecule is described by the time dependent Schrödinger equation (TDSE), rewritten in dimensionless form for generality: $i\hbar\frac{\partial}{\partial t}|\Phi\rangle = H(t)|\Phi\rangle$. In the case of nonresonant molecule and field interaction, the Hamiltonian $H(t)$ is the sum of the Hamiltonian of the free molecule H_0 and the potential induced by the electric field $H_{int}(t)$ as $H(t) = H_0 + H_{int}(t)$. In this expression, $H_0 = B\hat{J}^2$ with $H_0|JM >= BJ(J+1)\,|JM >$, where B is the rotational constant, $\hat{J}$ is the angular momentum operator, and $|JM >$ is the rotational eigenstate with the angular momentum quantum number J and its projection M onto the laser polarization direction [33].

The Hamiltonian takes the form $H(t) = B[(\hat{J}^2 - \omega_\perp(t)) - \Delta\omega(t)\cos^2\theta]$ for linearly polarized light with dimensionless interaction parameters $\omega_{||}(t) = \alpha_{||}E^2(t)/2B$, $\omega_\perp(t) = \alpha_\perp E^2(t)/2B$, and $\Delta\omega(t) = \omega_{||} - \omega_\perp$ [34,35].

By considering an initial state $|\Phi_{J_0M_0}(t)\rangle$, the rotational wave function can be written as the superposition of rotational wave packets [2,36], $|\Phi_{J_0M_0}(t)\rangle = \sum_{JM} d_{JM}^{J_0M_0}(t)\exp\left(-i\frac{E_J t}{\hbar}\right)|JM\rangle$, where $d_{JM}^{J_0M_0}(t)$ are the expansion coefficients determined by solving differential equations for linearly polarized light [35] as

$$\begin{aligned} i\tfrac{\hbar}{B}d'^{J_0M_0}_{JM}(t) &= d_{JM}^{J_0M_0}(t)\langle JM|(\hat{J}^2 - \omega_\perp(t))|JM\rangle \\ &\quad - \sum_{J'M'} d_{J'M'}^{J_0M_0}(t)\langle JM|\Delta\omega(t)\cos^2\theta|J'M'\rangle\exp\left(-\tfrac{i(E_{J'}-E_J)t}{\hbar}\right). \end{aligned} \tag{1}$$

The constant term in the Hamiltonian can be dropped for convenience due to not providing any torque; then taking account of the only term left that is angular dependent, the solution is written as the superposition of the rotational states $|JM\rangle$ by the selection rules $\Delta J = 0, \pm 2$ with the same parity, even or odd, and $\Delta M = 0$ [35]. For the linearly polarized light, the expression is given by [35,37,38]

$$\begin{aligned} i\tfrac{\hbar}{B}d'^{J_0M_0}_{JM}(t) &= -d^{J_0M_0}_{J-2,M_0}(t)\Delta\omega(t)\langle J,M_0|\cos^2\theta|J-2,M_0\rangle\exp(-i(E_{J-2}-E_J)t/\hbar) \\ &\quad -d^{J_0M_0}_{J,M_0}(t)\Delta\omega(t)\langle JM_0|\cos^2\theta|JM_0\rangle + d^{J_0M_0}_{JM_0}(t)(J(J+1)-\omega_\perp(t)) \\ &\quad -d^{J_0M_0}_{J+2,M_0}(t)\Delta\omega(t)\langle J,M_0|\cos^2\theta|J+2,M_0\rangle\exp(-i(E_{J+2}-E_J)t/\hbar). \end{aligned} \tag{2}$$

Here are the matrix elements [39,40]

$$\begin{aligned} \langle J,M_0|\cos^2\theta|J-2,M_0\rangle &= \frac{1}{2J-1}\sqrt{\frac{((J-1)^2-M_0^2)(J^2-M_0^2)}{(2J-3)(2J+1)}} \\ \langle JM_0|\cos^2\theta|JM_0\rangle &= \frac{1}{3}+\frac{2}{3}\left[\frac{J(J+1)-3M_0^2}{(2J-1)(2J+3)}\right] \\ \langle J,M_0|cos^2\theta|J+2,M_0\rangle &= \frac{1}{2J+3}\sqrt{\frac{((J+1)^2-M_0^2)((J+2)^2-M_0^2)}{(2J+1)(2J+5)}}. \end{aligned} \tag{3}$$

For a linear molecule with the initial state $|J_0M_0\rangle$ and the eigenvalue $E_J = BJ(J+1)$, $\langle\cos^2\theta\rangle$ can be written as

$$\begin{aligned}\left\langle\cos^2\theta\right\rangle_{J_oM_o}(t) &= \left\langle\Phi_{J_0M_0}(t)|\cos^2\theta|\Phi_{J_0M_0}(t)\right\rangle \\ &= \sum_J d^{J_0M_0^*}_{J-2,M_0}(t)d^{J_0M_0}_{JM_0}(t)\langle J,M_0|\cos^2\theta|J-2,M_0\rangle\exp(-iB(4J-2)t/\hbar) \\ &\quad+\sum_J |d^{J_0M_0}_{JM_0}(t)|^2\langle JM_0|\cos^2\theta|JM_0\rangle \\ &\quad+\sum_J d^{J_0M_0^*}_{J+2,M_0}(t)d^{J_0M_0}_{JM_0}(t)\langle J,M_0|\cos^2\theta|J+2,M_0\rangle\exp(-iB(4J+6)t/\hbar)\end{aligned} \tag{4}$$

By shifting $J \to J+2$ in the first term, the equation can be reorganized in a symmetric form,

$$\begin{aligned}\langle\cos^2\theta\rangle_{J_0M_0}(t) &= \sum_{J=2}^{J_{\max}} d^{J_0M_0^*}_{J-2,M_0}(t)d^{J_0M_0}_{JM_0}(t)\langle J,M_0|\cos^2\theta|J-2,M_0\rangle\exp(-iB(4J+6)t/\hbar) \\ &\quad+\sum_J |d^{J_0M_0}_{JM_0}(t)|^2\langle JM_0|\cos^2\theta|JM_0\rangle \\ &\quad+\sum_{J=0}^{J_{\max}} d^{J_0M_0^*}_{J+2,M_0}(t)d^{J_0M_0}_{JM_0}(t)\langle J,M_0|\cos^2\theta|J+2,M_0\rangle\exp(-iB(4J+6)t/\hbar)\end{aligned} \tag{5}$$

where $J_{\max}$ stands for the maximum number of excited states.

Before the interaction of the field with the molecule, the gas ensemble is assumed to be in thermal equilibrium with Boltzmann distribution at temperature T. In the quantum-mechanical approach, the ensemble is a statistical mixture of states $|J_0M_0\rangle$ with different angular momenta, where $J_0 = 0,\ 1,\ 2,\ ...$ and $M_0 = -J_0,\ -(J_0-1),\ ...,\ 0,\ ...(J_0-1),\ J_0$. The probabilities of $|J_0M_0\rangle$ states follow Boltzmann distribution $P_{J_0} \sim (2J_0+1)\exp(-E_{J_0}/kT)$, where E_{J_0} is the rotational energy of $|J_0M_0\rangle$state and k is the Boltzmann constant. The $(2J_0+1)$ term accounts for the degeneracy within a given J_0 state. For a complete description, the influence of nuclear spin of atoms constituting the molecule must be taken into account. Consequently, an additional factor g_{J_0} originating from the nuclear spin statistics appears in the Boltzmann distribution: $P_{J_0} \sim g_{J_0}(2J_0+1)\exp(-E_{J_0}/kT)$. Finally, the degree of alignment of an ensemble at temperature T can be written by averaging the different states over the Boltzmann distribution including nuclear spin statistics

$$\ll\cos^2\theta\gg(t) = \frac{\sum_{J_0}^{J_{\max}}\sum_{M_0=-J_0}^{J_0} <\cos^2\theta>_{J_0M_0}(t)g_{J_0}\exp(-BJ_0(J_0+1)/kT)}{\sum_{J_0}^{J_{\max}}\sum_{M_0=-J_0}^{J_0} g_{J_0}\exp(-BJ_0(J_0+1)/kT)}. \tag{6}$$

For the nitrogen molecule, $g_{J_0} = 6$ for even J's and $g_{J_0} = 3$ for odd J's [41,42]. The ratio of even to odd states is therefore 2:1 for nitrogen gas.

In our case, considering a random ensemble of diatomic molecules, molecular axis orientation with respect to an external axis in any angle has equal probability; hence the average of the squared orientation cosine takes the value $\ll\cos^2\theta\gg = 1/3$ [33]. Using density matrix formalism, which has two parts with diagonal and off-diagonal elements standing for populations and coherences, respectively, the expectation value of the molecular

alignment can be written as $\ll \cos^2\theta \gg = \ll \cos^2\theta \gg_P + \ll \cos^2\theta \gg_C$ where, $\ll \cos^2\theta \gg_P$ and $\ll \cos^2\theta \gg_C$ are calculated from Eq. (6) using

$$< \cos^2\theta >_P = \sum_J |d^{J_0M_0}_{JM_0}(t)|^2 \langle JM_0| \cos^2\theta |JM_0\rangle \tag{7}$$

and

$$\begin{aligned} < \cos^2\theta >_C = & \sum_{J=2}^{J_{\max}} d^{J_0M_0^*}_{J-2,M_0}(t) d^{J_0M_0}_{JM_0}(t) \langle J, M_0| \cos^2\theta |J-2, M_0\rangle \exp(-iB(4J+6)t/\hbar) \\ & + \sum_{J=0}^{J_{\max}} d^{J_0M_0^*}_{J+2,M_0}(t) d^{J_0M_0}_{JM_0}(t) \langle J, M_0| \cos^2\theta |J+2, M_0\rangle \exp(-iB(4J+6)t/\hbar), \end{aligned} \tag{8}$$

respectively. Figure 2 illustrates the total nonadiabatic molecular alignment and its decomposition into $\ll \cos^2\theta \gg_P$ and $\ll \cos^2 \gg_C$, where $\ll \cos^2 \gg_P$ probes the population and $\ll \cos^2\theta \gg_C$ measures the coherences.

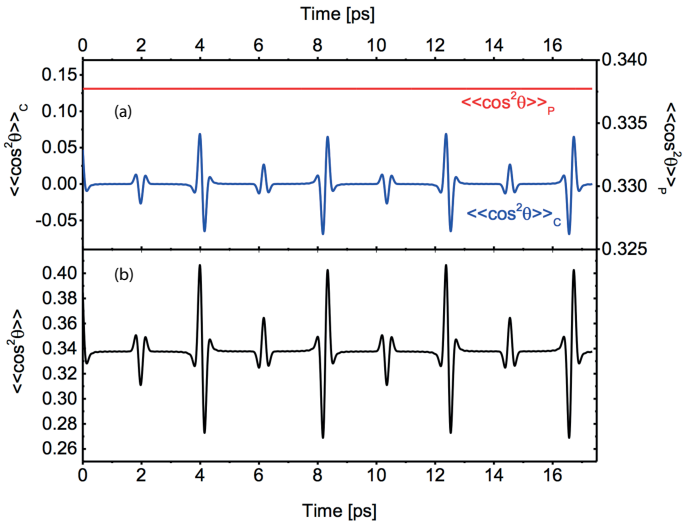

Figure 2. Calculations of the molecular alignment of N_2 at 300 K, induced by a Gaussian laser pulse with 50 fs FWHM and power of 1.3×10^{13} W/cm^2. (a) Alignment parameter decomposed into $\ll \cos^2(\theta) \gg_P$ and $\ll \cos^2(\theta) \gg_C$ (b) total $\ll \cos^2(\theta) \gg$.

The refractive index of a gas at moderate densities can be approximated using the Lorentz–Lorenz equation [43] as $n \approx 1 + 2\pi N < \alpha > (t)$, where N is the number density of molecules per unit volume and α is the polarizability. Here $< \alpha > (t) =< \hat{e} \cdot \alpha . \hat{e} > (t) =< e_i \alpha_{ij} e_j > (t)$, where $\hat{e}$ is the electric field polarization and α is the molecular polarizability tensor. For a linear molecule, where we choose the body-fixed axis z along the molecular axis, the only nonvanishing components of the molecular polarizability tensor α are $\alpha_{xx} = \alpha_{yy} = \alpha_\perp$ and $\alpha_{zz} = \alpha_{||}$. We take the molecular symmetry along the z-axis and so the electric field of the laser can be considered as $E = \hat{x}E_x + \hat{z}E_z$ for a particular molecular orientation. In the space-fixed field, for an ensemble of molecular orientations

$$\begin{aligned} n &= 1 + 2\pi N[< e_x^2 > (t)\alpha_{xx} + < e_z^2 > (t)\alpha_{zz}] \\ &= 1 + 2\pi N[\alpha_\perp < \sin^2\theta > + \alpha_{||} < \cos^2\theta >] \end{aligned} . \tag{9}$$

It becomes

$$n(t) = 1 + 2\pi N[\Delta\alpha < \cos^2\theta > (t) + \alpha_\perp], \tag{10}$$

where $\Delta\alpha = \alpha_{||} - \alpha_\perp$ and $e_z = \hat{e}\cdot\hat{z} = \cos\theta$ is the cosine of the angle between the electric field and the molecular axis (z).

The molecular ensemble before the pump pulse arrived is averaged over the solid angle and given by the expression $< \cos^2\theta > (t = -\infty) = 1/3$. Thus, the linear refractive index is

$$n(t = -\infty) = n_0 = 1 + 2\pi N(\frac{1}{3}\Delta\alpha + \alpha_\perp). \tag{11}$$

The degree of alignment of the ensemble at a rotational temperature T in thermal equilibrium $< \cos^2\theta > (t)$ is written by averaging the degree of alignment of a single rotational state (Eq. (6)) over the Boltzmann distribution as $\ll \cos^2\theta \gg (t)$. Therefore, the nonadiabatic molecular alignment leads to a periodic modulation with the change in the refractive index of a gas along the polarization direction of the aligning pulse and it is given by [7]

$$\Delta n_{||}(r,t) = n(t) - n_0 = \frac{2\pi N}{n_0}\Delta\alpha\left(\ll \cos^2\theta \gg (r,t) - \frac{1}{3}\right) \tag{12}$$

with $\ll \cos^2\theta \gg (r,t)$ the thermally averaged alignment expectation value.

On the other hand, the change in the refractive index considering the direction perpendicular to the field polarization is described by $\Delta n_\perp(t) = -\frac{1}{2}\Delta n_{||}(t)$ [44–46]:

$$\Delta n_\perp(r,t) = -\frac{1}{2}\Delta n_{||}(t) = -\frac{\pi N}{n_0}\Delta\alpha\left(\ll \cos^2\theta \gg (r,t) - \frac{1}{3}\right), \tag{13}$$

assuming that the plasma has inclination neither parallel nor perpendicular to the field polarization of the laser [47,48]. Then the resulted birefringence, the nonlinear refractive indices difference, $\Delta n(r,t)$ expressed as [49–51]

$$\begin{aligned} \Delta n_{align}(r,t) &= \Delta n_{||}(r,t) - \Delta n_\perp(r,t) \\ &= \tfrac{3\pi N}{n_0}\Delta\alpha(\langle\langle\cos^2\theta\rangle\rangle(r,t) - \tfrac{1}{3}), \end{aligned} \tag{14}$$

i.e. the change in the refractive index is proportional to the deviation of the alignment degree from the isotropic one, which equals 1/3.

Then, considering the polarization of the pump pulse is in the x direction and the propagation is in the z direction, for each polarization of the probe pulse, the refractive index modulation due to the electronic Kerr effect is given by the expression [52–54] $\Delta n_{Kerr,x}(t) = 2n_2 I_{pump}(t)$ and $\Delta n_{Kerr,y}(t) = \frac{1}{3}\Delta n_{Kerr,x}(t)$. The plasma contribution to the refractive index is given by [55] $\Delta n_{plasma}(t) = -\frac{2\pi e^2 N_e(t)}{m_e\omega_0^2}$, where ω_0 , $N_e(t)$, e, and m_e are the central angular frequency of the laser, electron density, and charge and mass of an electron, respectively. The pump had intensities too low to produce a filament and so the electronic Kerr effect and the plasma can be negligible. Therefore, we only considered the refractive index changes caused by the molecular alignment. On the other hand, the alignment produces a noticeable change in filament formation and white-light generation, when the amplitude of the change in the refractive index due to alignment $\Delta n_a = \Delta n(r,t)$ produced by the pump beam becomes comparable to the refractive index change owing to the optical Kerr

effect, $\Delta n_{Kerr} = n_2 I$, induced by the probe beam with intensity I. With $n_2(N_2) = 2.3 \times 10^{-19} cm^2/W$ and $I = 5 \times 10^{13} W/cm^2$ we obtain $\Delta n = 4.4 \times 10^{-5}$ for typical gas pressure 4 bars. A similar value of the magnitude of the refractive index variations due to alignment Δn_a follow from simulations for the pump pulse with intensity $I = 10^{13} W/cm^2$ and duration $\tau \approx 250 fs$, which fits well the experimental parameters. The additional contribution to the alignment caused by the alignment changes the self-focusing length: it is decreasing for the alignment and increasing for the antialignment, and thus the dynamics of the rotational wave packet change the filament formation and modulate the white-light generation.

4. Results and discussion

Experimentally, there is a correlation between the pressure of the environment and the index of refraction of the medium. High pressure leads to an increase in the index of refraction and supports the filamentation formation at much lower intensities. We can analyze the pressure dependence of the process recalling the alignment parameter of a gas $\ll \cos^2(\theta) \gg$ in terms of its components as $\ll \cos^2(\theta) \gg_p$ and $\ll \cos^2(\theta) \gg_c$ depending on the collisional dynamics of the system [56]. Before the pump pulse arrived, the rotational levels are in thermal equilibrium and so $\ll \cos^2(\theta) \gg_p = 1/3$ and $\ll \cos^2(\theta) \gg_c = 0$. After the laser interacts with the molecule, laser excitation creates a rotational wave packet, i.e. coherent superposition of the rotational states with a sharp rise of $\ll \cos^2(\theta) \gg_p$ from its isotropic value of 1/3 to a value depending on the laser intensity applied and a nonzero $\ll \cos^2(\theta) \gg_c$ due to coherences created by the interaction. In the case of the molecule being isolated, after the pulse turn-off $\ll \cos^2(\theta) \gg_p$ stays constant while $\ll \cos^2(\theta) \gg_c$ oscillates with a constant amplitude at the rotational period. On the other hand, in a dissipative medium $\ll \cos^2(\theta) \gg_p$ falls to its initial value of 1/3 and $\ll \cos^2(\theta) \gg_c$ goes to zero due to decoherence [56].

It is noted that the value of $\ll \cos^2(\theta) \gg_p$, related to the population decay rate, in a medium at the equilibrium 1/3 can be accepted as the baseline value of alignment depending on the gas pressure. Although the alignment period observed was the same for different pressures, population decay rate was increased with higher pressure by considering the baseline of the revival structure as seen in Figure 3a. The relative difference for the 4-bar and 1-bar pressures is 6%. Similarly, $\ll \cos^2(\theta) \gg_c$, the coherence between the revival events, is increased with higher pressure as seen in Figure 3b.

To better examine the collisional dynamics of the system, we also measured the white-light signal around half revival times of molecular N_2 and N_2 in Ar versus time as seen in Figure 4. Since we use white-light signal $\propto \Delta n_{align}$ for alignment monitoring, the refractive index change value from the time-dependent alignment can now be expressed as $\Delta n_{align} = \Delta n^p_{align} + \Delta n^c_{align}$. The blue curve with superimposed triangles and the black curve with superimposed full squares for nitrogen and nitrogen in argon, respectively, of Figure 4 show the experimentally measurable signal for Δn_{align}, which is proportional to $\ll \cos^2(\theta) \gg$. The revivals of the molecular alignment will be weaker with time and then disappear because of relaxation of the population and decoherence. The baselines of the signals are the population contribution Δn^p_{align}, which are shown as a green and red dotted-dashed curves for nitrogen and nitrogen in argon, respectively, and they increase suddenly from 1/3 for $\ll \cos^2(\theta) \gg_p$ once the laser pulse populates the rotational wave packet and then decays to its equilibrium value in the time scale of population relaxation under field-free condition [56].

The oscillatory curves with superimposed triangles and circles present the coherence contribution Δn^c_{align} for nitrogen and nitrogen with argon, which can be extracted from the signal using $\Delta n_{align} - \Delta n^p_{align}$. The

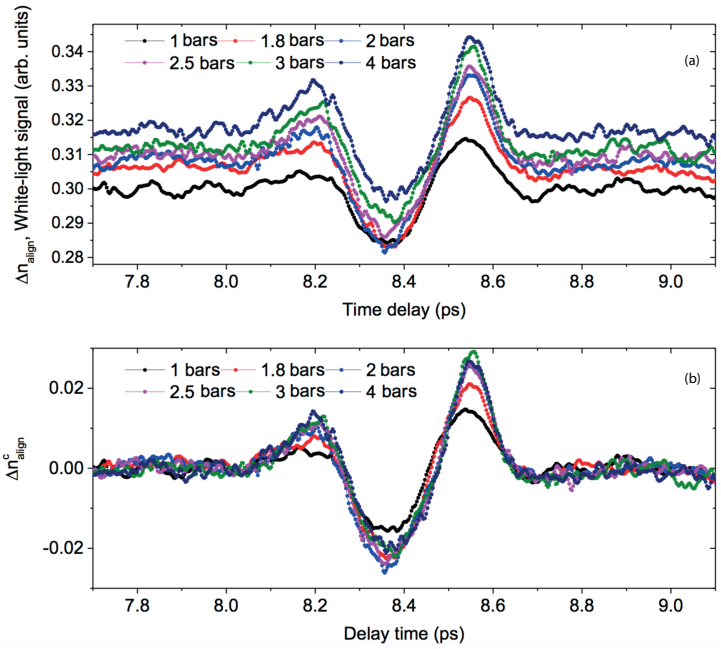

Figure 3. The nonadiabatic alignment pressure dependence: (a) The measured white-light signals and (b) the coherence contributions to the white-light signals for the different pressures from 1 bar to 4 bars.

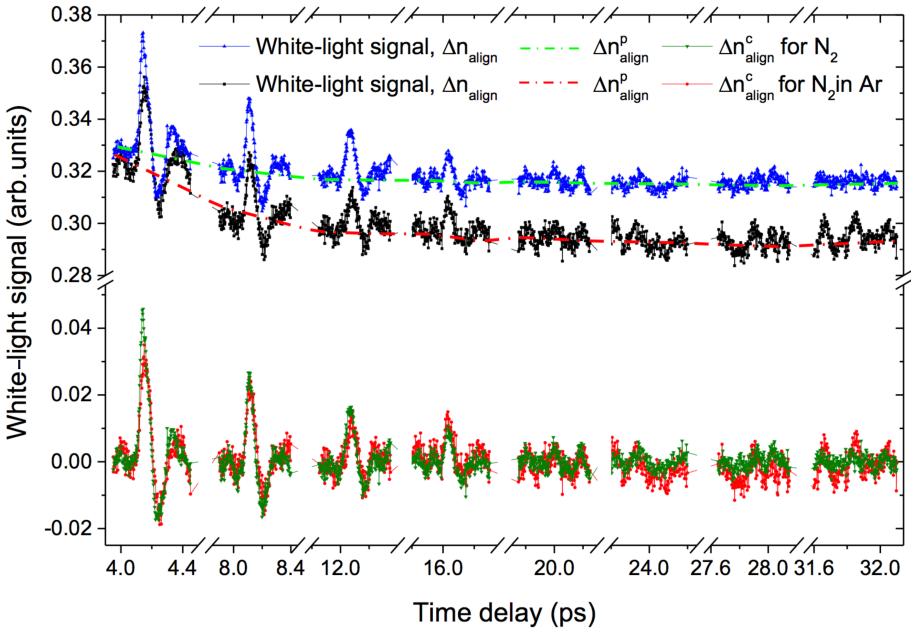

Figure 4. The measured white-light signal around half revival times of N_2 and N_2 in Ar versus time. To monitor field-free alignment, the white-light signal is used as an experimentally measurable signal for the refractive index change Δn_{align}, which is proportional to $\ll \cos^2 \gg$ and consists of two elements as $\Delta n_{align} = \Delta n^p_{align} + \Delta n^c_{align}$. The blue curve with superimposed triangles and the black curve with superimposed full squares represent the measured white-light signals for nitrogen and nitrogen in argon, respectively. The green curve with superimposed triangles and the red curve with superimposed full circles show the coherence contributions of the measured white-light signals and the green and red dotted-dashed curves show the population contribution as the baselines of the white-light signals for nitrogen and nitrogen in argon, respectively.

oscillations of laser-induced molecular alignment result from dephasing and rephrasing of coherences of molecular rotational dynamics in a dissipative environment.

5. Conclusion

By measuring laser-induced nonadiabatic alignment in nitrogen and mixtures of nitrogen with argon gas, we find that dissipative media produce desired alignment characteristics that can be used as a control tool of molecular dynamics in dissipative environments.

Acknowledgments

This work was supported by the Robert A. Welch Foundation Grant No. A1546. I am thankful to my colleagues N Kaya, J Strohaber, A Kolomenskii, and H Schuessler, who shared their knowledge and expertise that greatly assisted in this work.

References

[1] Kaya, G.; Kaya, N.; Strohaber, J.; Hart, N.; Kolomenskii, A.; Schuessler, H. *Appl. Phys. B* **2016**, *122*, 288.

[2] Stapelfeldt, H; Seideman, T. *Rev. Mod. Phy.* **2003**, *75*, 543-557.

[3] Seideman, T.; Hamilton, E. *Advances in Atomic, Molecular, and Optical Physics*; Academic Press: San Diego, CA, USA, 2005.

[4] Henrik, S., *Phy. Scr.* **2004**, *2004*, 132.

[5] Fleischer, S.; Averbukh, I. S.; Prior, Y. *Phys. Rev. A* **2006**, *74*, 041403.

[6] Itatani, J.; Levesque, J.; Zeidler, D.; Niikura, H.; Pepin, H.; Kieffer, J. C.; Corkum, P. B.; Villeneuve, D. M. *Nature* **2004**, *432*, 867-871.

[7] Bartels, R. A.; Weinacht, T. C.; Wagner, N.; Baertschy, M.; Greene, C. H.; Murnane, M. M.; Kapteyn, H. C. *Phys. Rev. Lett.* **2001**, *88*, 013903.

[8] Lee, K. F.; Villeneuve, D. M.; Corkum, P. B.; Shapiro, E. A. *Phy. Rev. Lett.* **2004**, *93*, 233601.

[9] Zewail, A. H. *J. Phys. Chem. A* **2000**, *104*, 5660-5694.

[10] Loriot, V.; Hertz, E.; Lavorel, B.; Faucher, O. *J. Phys. B At. Mol. Opt. Phys.* **2008**, *41*, 015604.

[11] Litvinyuk, I. V.; Lee, K. F.; Dooley, P. W.; Rayner, D. M.; Villeneuve, D. M.; Corkum, P. B., *Phys. Rev. Lett.* **2003**, *90*, 233003.

[12] Kaya, N.; Kaya, G.; Strohaber, J.; Kolomenskii, A. A.; Schuessler, H. A. *Eur. Phys. J. D* **2016**, *70*, 224.

[13] Kenzo, M.; Takayuki, S.; Didier, N., *J. Phys. B At. Mol. Opt. Phys.* **2004**, *37*, 753.

[14] Dooley, P. W.; Litvinyuk, I. V.; Lee, K. F.; Rayner, D. M.; Spanner, M.; Villeneuve, D. M. Corkum, P. B., *Phys. Rev. A* **2003**, *68*, 023406.

[15] Velotta, R.; Hay, N.; Mason, M. B.; Castillejo, M.; Marangos, J. P. *Phys. Rev. Lett.* **2001**, *87*, 183901.

[16] Kanai, T.; Minemoto, S.; Sakai, H. *Nature* **2005**, *435*, 470-474.

[17] Vozzi, C.; Calegari, F.; Benedetti, E.; Caumes, J. P.; Sansone, G.; Stagira, S.; Nisoli, M.; Torres, R.; Heesel, E.; Kajumba, N.; et al. *Phys. Rev. Lett.* **2005**, *95*, 153902.

[18] Sayrac, M.; Kolomenskii, A. A.; Anumula, S.; Boran, Y.; Hart, N. A.; Kaya, N.; Strohaber, J.; Schuessler, H. A. *Rev. Sci. Instrum.* **2015**, *86*, 043108.

[19] Ripoche, J. F.; Grillon, G.; Prade, B.; Franco, M.; Nibbering, E.; Lange, R.; Mysyrowicz, A. *Opt. Commun.* **1997**, *135*, 310-314.

[20] Calegari, F.; Vozzi, C.; Gasilov, S.; Benedetti, E.; Sansone, G.; Nisoli, M.; De Silvestri, S.; Stagira, S. *Phys. Rev. Lett.* **2008**, *100*, 123006.

[21] Varma, S.; Chen, Y. H.; Palastro, J. P.; Fallahkair, A. B.; Rosenthal, E. W.; Antonsen, T.; Milchberg, H. M. *Phys. Rev. A* **2012**, *86*, 023850.

[22] Kaya, N.; Kaya G.; Sayrac, M.; Boran, Y.; Anumula, S.; Strohaber, J.; Kolomenskii, A. A.; Schuessler, H. A. *Opt. Express* **2016**, *24*, 2562-2576.

[23] Kolomenskii, A. A.; Strohaber, J.; Kaya, N.; Kaya, G.; Sokolov, A. V.; Schuessler, H. A. *Opt. Express* **2016**, *24*, 282-293.

[24] Felker, P. M. *J. Phys. Chem. A* **1992**, *96*, 7844-7857.

[25] Heritage, J. P.; Gustafson, T. K.; Lin, C. H. *Phys. Rev. Lett.* **1975**, *34*, 1299-1302.

[26] Henriksen, N. E. *Chem. Phys. Lett.* **1999**, *312*, 196-202.

[27] Seideman, T. *Phys. Rev. Lett.* **1999**, *83*, 4971-4974.

[28] Rosca-Pruna, F.; Vrakking, M. J. J. *Phys. Rev. Lett.* **2001**, *87*, 153902.

[29] Renard, V.; Renard, M.; Guérin, S.; Pashayan, Y. T.; Lavorel, B.; Faucher, O.; Jauslin, H. R. *Phys. Rev. Lett.* **2003**, *90*, 153601.

[30] Rouzée, A.; Guérin, S.; Faucher, O. ; Lavorel, B. *Phys. Rev. A* **2008**, *77*, 043412.

[31] Bustard, P. J.; Lausten, R.; Sussman, B. J. *Phys. Rev. A* **2012**, *86*, 053419.

[32] Kaya, N. *Turk. J. Phys.* **2017**, *41*, 196-202.

[33] Owschimikow, N.; Schmidt, B.; Schwentner, N. *Phys. Rev. A* **2009**, *80*, 053409.

[34] Friedrich, B.; Herschbach, D. *J. Chem. Phys.* **1999**, *111*, 6157-6160.

[35] Ortigoso, J.; Rodrıguez, M.; Gupta, M.; Friedrich, B. *J. Chem. Phys.* **1999**, *110*, 3870-3875.

[36] Faisal, F. H. M.; Abdurrouf, A. *Phys. Rev. Lett.* **2008**, *100*, 123005.

[37] Ben Haj-Yedder, A.; Auger, A.; Dion, C. M.; Cancès, E.; Keller, A.; Le Bris, C.; Atabek, O. *Phys. Rev. A* **2002**, *66*, 063401.

[38] Hamilton, E.; Seideman, T.; Ejdrup, T.; Poulsen, M. D.; Bisgaard, C. Z.; Viftrup, S. S.; Stapelfeldt, H. *Phys. Rev. A* **2005**, *72*, 043402.

[39] Varshalovich, D. A.; Moskalev, A. N.; Khersonskii, V. K. *Quantum Theory of Angular Momentum: Irreducible Tensors, Spherical Harmonics, Vector Coupling Coefficients, 3nj Symbols*. World Scientific Pub.: Singapore, 1988.

[40] Zare, R. N. *Angular Momentum: Understanding Spatial Aspects in Chemistry and Physics*; Wiley: New York, NY, USA, 1988.

[41] McQuarrie, D. A; Simon, J. D. *Physical Chemistry: a Molecular Approach*. University Science Books: Sausalito, CA, USA, 1997.

[42] Bransden, B. H.; Joachain, C. J. *Physics of Atoms and Molecules*. Prentice Hall: Upper Saddle River, NJ, USA, 2003.

[43] Born, M.; Wolf, E.; Bhatia, A. B.; Gabor, D.; Stokes, A. R.; Taylor, A. M.; Wayman, P. A.; Wilcock, W. L. *Principles of Optics: Electromagnetic Theory of Propagation, Interference and Diffraction of Light*. Cambridge University Press: Cambridge, UK, 2000.

[44] Hoque, M. Z.; Lapert, M.; Hertz, E.; Billard, F.; Sugny, D.; Lavorel, B.; Faucher, O. *Phys. Rev. A* **2011**, *84*, 013409.

[45] Houzet, J.; Billard, F.; Hertz, E.; Chateau, D.; Chaussard, F.; Lavorel, B.; Faucher, O. *Appl. Phys. B* **2012**, *108*, 897-902.

[46] Hertz, E.; Daems, D.; Guérin, S.; Jauslin, H. R.; Lavorel, B.; Faucher, O. *Phys. Rev. A* **2007**, *76*, 043423.

[47] Wahlstrand, J. K.; Milchberg, H. M., *Opt. Lett.* **2011**, *36*, 3822-3824.

[48] Odhner, J. H.; Romanov, D. A.; McCole, E. T.; Wahlstrand, J. K.; Milchberg, H. M.; Levis, R. J. *Phys. Rev. Lett.* **2012**, *109*, 065003.

[49] Varma, S.; Chen, Y. H.; Milchberg, H. M. *Phys. Rev. Lett.* **2008**, *101*, 205001.

[50] Chen, Y. H.; Varma, S.; York, A.; Milchberg, H. M. *Opt. Express* **2007**, *15*, 11341-11357.

[51] Yuan, S.; Li, M.; Feng, Y.; Li, H.; Zheng, L.; Chin, S. L.; Zeng, H. *J. Phys. B: At. Mol. Opt. Phys.* **2015**, *48*, 094018.

[52] Béjot, P.; Petit, Y.; Bonacina, L.; Kasparian, J.; Moret, M.; Wolf, J. P. *Opt. Express* **2008**, *16*, 7564-7570.

[53] Marceau, C.; Ramakrishna, S.; Génier, S.; Wang, T. J.; Chen, Y.; Théberge, F.; Châteauneuf, M.; Dubois, J.; Seideman, T.; Chin, S. L. *Opt. Commun.* **2010**, *283*, 2732-2736.

[54] Agrawal, G. P. *Nonlinear Fiber Optics*; Academic Press: San Diego, CA, USA, 2006.

[55] Chin, S. L.; Hosseini, S. A.; Liu, W.; Luo, Q.; Théberge, F.; Aközbek, N.; Becker, A.; Kandidov, V. P.; Kosareva, O. G.; Schroeder, H. *Can. J. Phys.* **2005**, *83*, 863-905.

[56] Ramakrishna, S.; Seideman, T. *J. Chem. Phys.* **2006**, *124*, 034101.